Leading Edge

Primer

Cell

Breaking the Diffraction Barrier: Super-Resolution Imaging of Cells

Bo Huang,[1] Hazen Babcock,[2] and Xiaowei Zhuang[2,3,*]
[1]Department of Pharmaceutical Chemistry and Department of Biochemistry and Biophysics, University of California, San Francisco, San Francisco, CA 94158, USA
[2]Center for Brain Science
[3]Howard Hughes Medical Institute and Department of Chemistry and Chemical Biology and Department of Physics
Harvard University, Cambridge, MA 02138
*Correspondence: zhuang@chemistry.harvard.edu

Anyone who has used a light microscope has wished that its resolution could be a little better. Now, after centuries of gradual improvements, fluorescence microscopy has made a quantum leap in its resolving power due, in large part, to advancements over the past several years in a new area of research called super-resolution fluorescence microscopy. In this Primer, we explain the principles of various super-resolution approaches, such as STED, (S)SIM, and STORM/(F) PALM. Then, we describe recent applications of super-resolution microscopy in cells, which demonstrate how these approaches are beginning to provide new insights into cell biology, microbiology, and neurobiology.

For centuries, light microscopy has greatly facilitated our understanding of how cells function. In fact, entire fields of biology have emerged from images acquired under light microscopes. For instance, more than 300 hundred years ago, Antonie van Leeuwenhoek used his self-ground optical lenses to discover bacteria and commence the field of microbiology. Then, ~200 years later, Ramón y Cajal used light microscopes to visualize Golgi-stained brain sections and create beautiful drawings of neurons, which led to his ingenious vision of how information flows in the nervous systems and helped to form modern neurobiology.

Indeed, one major element that makes light microscopy so powerful in biological research is the development of various staining methods that permit the labeling of specific molecules and cells. For example, fluorescence in situ hybridization (FISH) detects DNA and RNA molecules with specific sequences, whereas immunofluorescence labels and fluorescent proteins allow the imaging of particular proteins in cells (Giepmans et al., 2006). Even single molecules within a living cell can be visualized when these labeling strategies are combined with highly sensitive optical schemes and detectors (Lord et al., 2010; Xie et al., 2008).

The unrivaled combination of molecule-specific contrast and live-cell imaging capability makes fluorescence microscopy the most popular imaging modality in cell biology. Browse through any cell biological journal, and the impact of fluorescent microscopy is obvious, with > 80% of the images of cells in the book usually acquired with a fluorescent microscope. However, the application of fluorescence microscopy to many areas of biology is still hindered by its moderate resolution of several hundred nanometers. This resolution is approximately the size of an intracellular organelle and thus is inadequate for dissecting the inner architecture of many subcellular structures.

The resolution for optical microscopy is limited by the diffraction, or the "spreading out," of the light wave when it passes through a small aperture or is focused to a tiny spot. Because this property is intrinsic to all waves, breaking the diffraction barrier of light microscopy has been deemed impossible for a long time. However, such limitations have not deterred a small group of scientists from pursuing "super-resolution" fluorescence microscopy that breaks through this seemingly impenetrable barrier.

The risk has paid off abundantly. Recently, these research teams have developed several optical microscopy techniques that have shattered the diffraction barrier, improving spatial resolution by an order of magnitude or more over the diffraction limit. Most importantly, these techniques are beginning to provide insights into biological processes at the cellular and molecular scale that were hitherto unattainable. In this Primer, we review the technological advances in the burgeoning field of "super-resolution fluorescence microscopy." Then, we describe the application of these techniques to various areas of biology, which have quickly demonstrated the great promise of this exciting new area of bioimaging.

Beating the Diffraction Limit of Resolution

When light is focused by the objective of a microscope, the notion of light "rays" converging to an infinitely sharp "focal point" does not happen. Instead, the light wave forms a blurry focal spot with a finite size due to diffraction (Figure 1A). The size of the spot depends on the wavelength of the light and the angle at which the light wave converges; the latter is, in turn, determined by the numerical aperture of the objective. The width of the spot is $\sim 0.6\, \lambda/NA$, wherein λ is the wavelength of the light and NA is the numerical aperture of the lens. Similarly, a point emitter, such as a single fluorescent molecule,
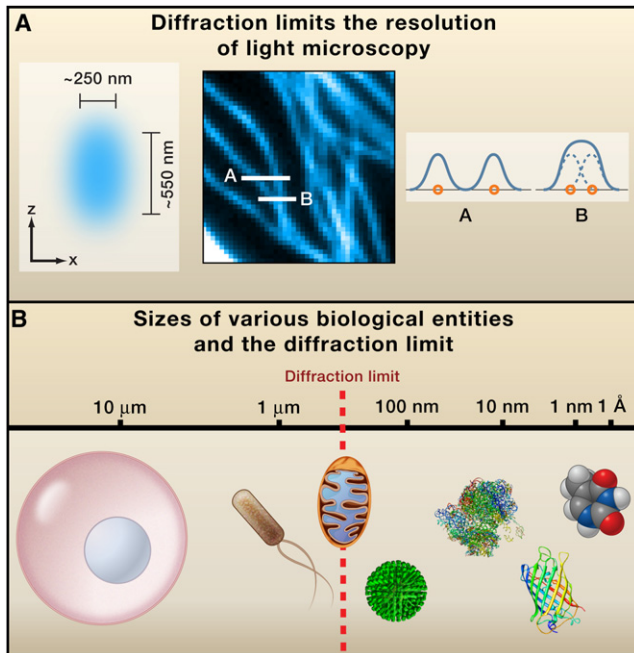
Figure 1. Diffraction-Limited Resolution of Conventional Light Microscopy

(A) The focal spot of a typical objective with high numerical aperture, depicted by the cyan ellipsoid, has a width of ∼250 nm in the lateral directions and ∼550 nm in the axial direction. The image of a point emitter imaged through the objective, namely the point spread function, also has similar widths. These widths define the diffraction-limited resolution. Two objects separated by a distance larger than this resolution limit appear as two separate entities in the image. Otherwise, they appear as a single entity (i.e., unresolvable). These two cases are exemplified by the two cross sections of the microtubule image, cyan curves A and B in the right panel, at the corresponding positions indicated by the white lines in the middle panel.

(B) The size scale of various biological structures in comparison with the diffraction-limited resolution. (Left to right) A mammalian cell, a bacterial cell, a mitochondrion, an influenza virus, a ribosome, the green fluorescent protein, and a small molecule (thymine).

also appears as a blurry spot with a finite size when imaged through a microscope. The intensity profile of this spot, which defines the point spread function (PSF) of the microscope, has approximately the same width as that of the focal spot described above. Consequently, two identical emitters separated by a distance less than the width of the PSF will appear as a single object, making them unresolvable from each other (Figure 1A).

This resolution limit was originally recognized by Ernst Abbe ∼150 years ago, and thus, it is also called the Abbe limit (Abbe, 1873). The diffraction-limited image resolution of objective lens with a high numerical aperture is ∼250 nm perpendicular to the direction of light propagation (i.e., in the lateral dimensions) and ∼550 nm parallel to the direction of light propagation (i.e., in the axial dimension) (Figure 1A). Many subcellular structures are smaller than these resolution limits, and therefore, they are unresolvable by light microscopes (Figure 1B).

For many years, several imaging techniques have pushed the boundary of the diffraction limit of light microscopy. Among these methods, confocal microscopy and multiphoton fluores-

cence microscopy not only enhance the image resolution, but also reduce the out-of-focus fluorescence background, allowing optical sectioning and thus three-dimensional imaging. In addition, infrared light experiences a lower amount of scattering from tissues, allowing deep tissue imaging with two-photon microscopy (Zipfel et al., 2003). 4Pi microscopy and I^{5}M use two opposing objective lenses to increase the effective numerical aperture of the microscope and thereby improve the image resolution (Gustafsson et al., 1995; Hell and Stelzer, 1992; Hell, 2003). Although these methods significantly improve the resolution, they are still fundamentally limited by diffraction and have, in practice, achieved resolutions of ∼100 nm in all three dimensions (Hell, 2003).

The diffraction-limited resolution applies only to light that has propagated for a distance substantially larger than its wavelength (i.e., in the far field). Therefore, one route to bypass this constraint is to place the excitation source or detection probe (usually an optical fiber, a metal tip, or simply a small aperture) near the sample (i.e., in the near field) (Synge, 1928). Indeed, near-field microscopy has achieved resolution substantially below 100 nm (Betzig et al., 1986; Lewis et al., 1984; Novotny and Hecht, 2006; Pohl et al., 1984). However, the requirement that the excitation source or detection probe be physically close to the target object (often within tens of nanometers) has made it difficult to look "into" a cell or a piece of tissue with near field microscopy, limiting the applications of this technique in biology.

It was not until recently that several novel fluorescence microscopy approaches completely shattered the diffraction limit of image resolution in the far field. In general, all of these approaches generate "diffraction-unlimited images" by using the physical properties of fluorescent probes to distinguish emissions from two nearby molecules within a diffraction-limited region. These super-resolution approaches can be divided into two primary classes. The first category is ensemble imaging approaches that use patterned illumination to spatially modulate the fluorescence behavior of molecules within a diffraction-limited region, such that not all of them emit simultaneously, thereby achieving subdiffraction limit resolution. This category includes stimulated emission depletion (STED) microscopy (Hell and Wichmann, 1994; Klar and Hell, 1999) and the related RESOLFT technology (Hofmann et al., 2005), as well as saturated structured illumination microscopy (SSIM) (Gustafsson, 2005; Heintzmann et al., 2002). The second category takes advantages of single-molecule imaging, using photoswitching or other mechanisms to stochastically activate individual molecules within the diffraction-limited region at different times. Images with subdiffraction limit resolution are then reconstructed from the measured positions of individual fluorophores. This second class has been termed stochastic optical reconstruction microscopy (STORM) (Rust et al., 2006), photoactivated localization microscopy (PALM) (Betzig et al., 2006), and fluorescence photoactivation localization microscopy (FPALM) (Hess et al., 2006).

Although these two categories of methods use different approaches to accomplish subdiffraction resolution, these techniques also share important commonalities. In both cases, a physical or chemical property of the fluorophore is used to maintain neighboring molecules in different states (i.e., "on"

and "off"), enabling them to be resolved from each other (Hell, 2007).

Super-Resolution Fluorescence Microscopy by Patterned Illumination

In this category of techniques, a patterned field of light is applied to the sample to manipulate its fluorescence emission. This spatial modulation can be implemented either in a "positive" or "negative" manner. In the positive case, the light field used to excite the sample and generate fluorescence is directly patterned. In contrast, the negative patterning approach enlists the help of an additional patterned light field to suppress the population of molecules that can fluoresce in the sample. In both of these approaches, the spatial information encoded into the illumination pattern allows neighboring fluorophores to be distinguished from each other, leading to enhanced spatial resolution.

Negative Patterning: STED and RESOLFT Microscopy

In STED microscopy, the patterned illumination prevents fluorophores from emitting light (Hell, 2007; Hell and Wichmann, 1994; Klar and Hell, 1999). This suppression is achieved by stimulated emission, a process in which a light source, called the depletion light, brings an excited fluorophore down to the lowest energy state (i.e., the ground state) before it can emit fluorescence signal. In practice, the depletion light is applied as a pattern surrounding the focal spot of the excitation laser. This reduces the size of the region of molecules that fluoresce, as if the "focal spot" of the microscope is sharpened (Figure 2A). Scanning this sharpened spot across a sample then allows a super-resolution image to be recorded. Thus, this negative patterning approach elegantly generates a positive image without the need of any postacquisition processing.

It is important to note that the depletion light pattern itself is created by the same diffraction-limited optics. Therefore, if the fluorophores respond to the depletion light in a linear manner, the resolution enhancement would be rather limited. STED microscopy surpasses this limit by taking advantage of the saturated response of fluorophores: once the depletion laser intensity is above the saturation level, the number of fluorophores remaining in the excited state (and thus capable of generating fluorescence) approaches zero. Thus, when a ring-shaped depletion light pattern with peak intensity significantly above the saturation level is applied to the sample, only the molecules within a small region near the center of the ring can generate fluorescence (Figure 2A). The size of this region, and thus the resolution of the microscope, scales approximately with the inverse square root of the intensity of the depletion light (or $\delta \approx \Delta / \sqrt{1 + I_{dep}/I_{sat}}$, wherein δ is the resolution, Δ is the diffraction-limited focal spot size, measured as the full width at half maximum intensity, and I_{dep} is the intensity of the depletion laser) (Hell, 2007).

In principle, this approach allows unlimited resolution improvement given an infinitely strong depletion light source. In practice, a number of factors influence the resolution of STED microscopy, including aberrations in the optics, scattering from the sample, and the photostability of the fluorophores. STED microscopy has reached a remarkable resolution of 6 nm using strong depletion intensity to image fluorescent defects in diamonds, which almost never photobleach (Rittweger et al.,
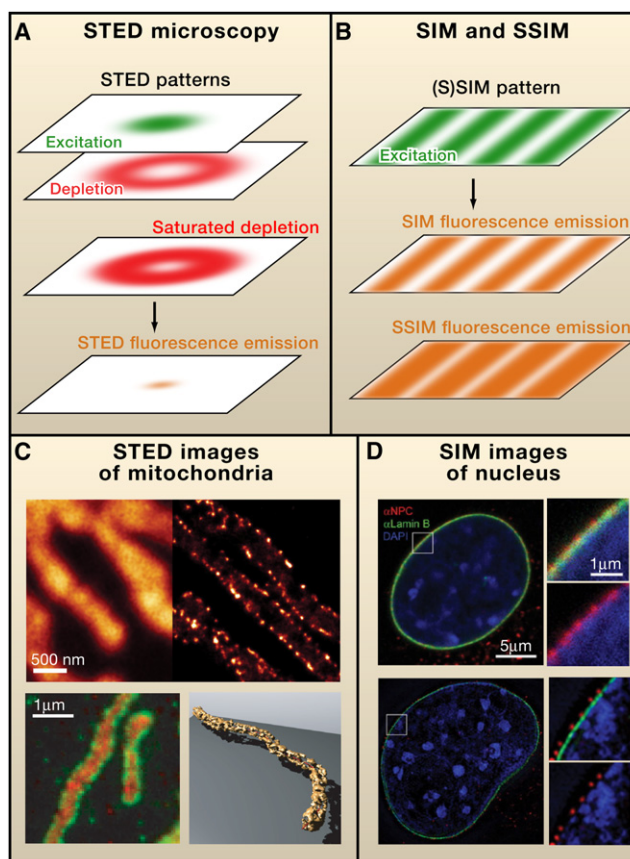

Figure 2. Super-Resolution Fluorescence Microscopy by Patterned Illumination

(A) In stimulated emission depletion (STED) microscopy, fluorophores are excited by a focused light beam (green, top layer), and an additional depletion light beam (red, second layer) is used to bring molecules back to the ground state by a process called stimulated emission. The intensity profile of this additional beam at the focal plane typically has a ring shape, depleting the population of molecules that can generate fluorescence, especially near the edge of the focal spot. The depletion efficiency can be described by the red pattern shown in the third layer when the depletion light intensity is above the saturation level. This depletion effect substantially reduces the size of the fluorescent spot (orange, bottom layer), thereby improving the image resolution.

(B) Structured illumination microscopy (SIM) and saturated SIM (SSIM) use pattered illumination to excite the sample and generate fluorescence. This patterned excitation typically has a sinusoidal shape (green, top layer). Such illumination generates a similarly shaped fluorescence emission pattern when the fluorescence responds in a linear manner (orange, middle layer). With strong excitation, fluorescence saturates, generating a saturated emission profile with narrow dark regions (orange, bottom layer) that provide spatial information substantially beyond the diffraction limit.

(C) Examples of STED images. (Top) Comparison between confocal (left) and STED (right) images of the outer membrane of mitochondria that is immunolabeled against the protein TOM20. Shown in the STED panel is an xy cross section of the 3D isoSTED image. (Bottom-left) Two-color isoSTED image of TOM20 (green) and the matrix protein HSP70 (red). (Bottom-right) Three-dimensional rendering of an isoSTED image of TOM20. Reprinted by permission from Macmillan Publishers Ltd: *Nature Methods* Schmidt et al., 2008. Reprinted with permission from Schmidt et al., 2009, American Chemical Society.

(D) Examples of 3D SIM images. (Top) Central cross-section of a confocal image of the nucleus stained for DNA, lamin B, and the nuclear pore complex. DNA (blue) is stained with DAPI. Lamin B (green) and the nuclear pore complex (red) are immunostained. The right panels show the magnified images of the boxed region in the left panel. (Bottom) 3D SIM images of a similarly stained nucleus. From Schermelleh et al., 2008. Reprinted with the permission from AAAS.

2009). On biological samples, STED imaging has achieved a resolution of 20 nm when using organic dyes and 50–70 nm resolution when using fluorescent proteins (http://www.mpibpc.mpg.de/groups/hell/STED_Dyes.html).

In addition to stimulated emission, other saturable optical transitions that send the molecule to dark states can also be used to shrink the area of molecules that fluoresce in a focal spot (Bretschneider et al., 2007; Hofmann et al., 2005). This extension of the STED approach, called reversible saturable optically linear fluorescence transitions (RESOLFT) microscopy, allows super resolution to be implemented with a substantially lower-depletion light intensity, causing less damage to delicate biological samples (Hell, 2007; Hofmann et al., 2005).

Positive Patterning: Structured Illumination Microscopy
Structured illumination microscopy (SIM) improves image resolution by using positive patterning of the excitation light (Heintzmann and Gustafsson, 2009), which is typically a sinusoidal pattern created by combining (i.e., interfering) two light beams. As the result, an image snapshot of the sample becomes the product of the sample structure itself and this excitation pattern (Figure 2B). A final image is then computationally reconstructed from multiple snapshots collected by scanning and rotating the pattern. In this process, the additional spatial modulation from the excitation pattern brings enhanced spatial resolution into the reconstructed image (Gustafsson, 2000; Heintzmann and Cremer, 1999).

As is true for the depletion light pattern used in STED, the illumination pattern created by interference is also limited by diffraction. Therefore, when the fluorescence signal scales linearly with the intensity of the excitation light, SIM results only in a doubling of spatial resolution (Figure 2B), which is ~100 nm in the lateral dimensions(Gustafsson, 2000).

Like with the negative patterning approach, the saturating response of the fluorophore can also be exploited here to further enhance the resolution (Gustafsson, 2005; Heintzmann et al., 2002). With sufficiently strong excitation, the fluorescence emission from a fluorophore will saturate. Saturated SIM (SSIM) utilizes this phenomenon to create sharp dark regions where the excitation pattern has zero intensity, providing image resolution significantly beyond the diffraction limit (Figure 2B). With this approach, a resolution of 50 nm has been obtained for imaging fluorescence microspheres (Gustafsson, 2005).

Fluorescent Probes
The basic form of SIM (i.e., the linear form) does not rely on any special photophysics of the fluorophores but purely on the optics of the microscope. Therefore, any fluorescent probe that is compatible with conventional fluorescence imaging is compatible with SIM. In addition, multicolor imaging can be achieved with SIM as it is with conventional fluorescence microscopy. Up to four colors can be imaged in the visible to near infrared (IR) spectrum range without incurring much crosstalk between the different color channels. As an example, Figure 2D shows a three-color SIM image of DNA, lamin B, and nuclear pore complexes in the nucleus (Schermelleh et al., 2008). In contrast, SSIM requires special fluorophores that have high photostability because the fluorophores are maintained in the highly reactive excited state most of the time in this imaging scheme.

STED microscopy can also use a wide range of existing fluorescent probes because all fluorophores can undergo stimulated emission (http://www.mpibpc.mpg.de/groups/hell/STED_Dyes.html). In practice, dyes that are photostable under a strong depletion light, such as Atto 647N, Atto 590, and Atto 565, provide greater resolution enhancement. Fluorescent proteins such as enhanced yellow fluorescent protein (EYFP) and Citrine have also been used. However, multicolor imaging with STED is less flexible compared to conventional fluorescence microscopy. To image one fluorophore, STED microscopy requires two lasers at the opposite ends of the absorption and emission spectra of the fluorophore for excitation and depletion, respectively. Therefore, the number of colors that can fit into the visible to near IR spectrum range is limited, and a maximum of two colors has been imaged simultaneously thus far (Donnert et al., 2007; Schmidt et al., 2008). Figure 2C shows a two-color STED image of the mitochondrial outer-membrane protein TOM20 and matrix protein HSP70 obtained using the latter approach (Schmidt et al., 2008).

Three-Dimensional Imaging
The depletion pattern in STED microscopy is created by inserting a spatial light modulator in the laser beam before it enters the microscope. As a ring-shaped pattern in the x-y plane improves the lateral resolution, a pattern having two maxima along the z axis improves the axial resolution (Hell, 2003). Overlaying these two patterns improves the resolution in both lateral and axial directions (Harke et al., 2008), allowing three-dimensional (3D) super-resolution imaging with a z resolution ~2.5 times the xy resolution. Subsequently, isoSTED has been realized with the z depletion pattern generated by two opposing objectives using the 4Pi configuration, reaching a resolution as high as ~30 nm in all three dimensions, as demonstrated by the 3D images of mitochondria shown in Figure 2C (Schmidt et al., 2008, 2009). Recently, STED microscopy has also been demonstrated with two-photon excitation, allowing super-resolution imaging deep into tissue samples (Ding et al., 2009; Moneron and Hell, 2009).

In SIM, a 3D illumination pattern can be created by the interference of three excitation light beams. Similar to the 2D counterpart, 3D SIM can double the resolution in all three dimensions, resulting in ~100 nm resolution in the lateral directions and ~300 nm in the axial direction (Gustafsson et al., 2008; Schermelleh et al., 2008). Figure 2D shows such a 3D SIM image of the nucleus. This 3D illumination pattern can be further combined with I^{5}M using two-opposing objectives to achieve an isotropic resolution of ~100 nm in all three dimensions (Gustafsson et al., 2008). 3D SSIM has not yet been implemented.

Live Imaging
For imaging dynamic events in living systems, time resolution is critical. In all imaging methods, there is an intrinsic trade-off between spatial and temporal resolution. This trade-off can be best understood from the Nyquist sampling theory. In the case of STED microscopy, which acquires an image by scanning the focal spot across the sample, the Nyquist criterion requires the scanning step size to be smaller than half of the desired resolution. The time resolution is then determined by the integration time per scanning step, the scanning step size, and the size of the imaging field. Better spatial resolution requires a smaller

scanning step size and, consequently, a longer time to image the same field of view.

Therefore, to achieve high temporal resolution, a small field of view and a relative large spatial resolution can be used. For example, impressive video rate STED imaging (28 frames per second) with 62 nm spatial resolution has been demonstrated in a field of view of $\sim$5 μm^2, allowing the motion of individual synaptic vesicles in a dendritic spine to be followed (Westphal et al., 2007). More recently, replacing the traditional pulsed lasers in STED microscopy with continuous wave lasers permits substantially faster scanning and thus higher time resolution (Willig et al., 2007). Using this scheme, a $\sim$70 μm^2 image of the endoplasmic reticulum took only 0.19 s to acquire (Moneron et al., 2010).

To study very fast processes, STED microscopy can be combined with fluorescence correlation spectroscopy (FCS). FCS is traditionally used with confocal microscopy to probe the movement or dynamics of molecules by monitoring the fluctuation of the fluorescence signal. The smaller detection region in STED enables FCS to probe dynamics at a much smaller length scale. Indeed, STED-FCS has been used to monitor diffusion dynamics with microsecond time resolutions and at a length scale as small as 20 nm (Eggeling et al., 2009).

SIM acquires an image by scanning an illumination pattern that covers the entire image field. Thus, the image acquisition time of SIM is limited by how fast the illumination pattern can be modulated and by how fast the camera can read out a snapshot. For 2D SIM, which requires nine different illumination patterns to reconstruct a resolution-enhanced image, a time resolution of $\sim$0.1 s has been demonstrated for live-cell imaging (Kner et al., 2009). Therefore, SIM is excellent for live-cell applications that require a large view field but not very high spatial resolution. Although live-cell imaging has not yet been demonstrated with SSIM, one would expect it to have higher spatial resolution at the cost of lower time resolution, as compared to SIM, because more illumination patterns are required to reconstruct an SSIM image (Gustafsson, 2005).

Super-Resolution Fluorescence Microscopy by Single-Molecule Switching
Localizing Single Molecules with High Precision
Fundamentally, a molecular assembly is defined by the coordinates for each of its constituents. Therefore, if we could image each molecule individually and determine its position with high precision, we could reconstruct a high-resolution image of the assembly. After 20 years of development in the field of single-molecule imaging (Moerner, 2007), single fluorophores are now routinely detected in a variety of imaging modalities, such as epifluorescence, total-internal-reflection, confocal, and multi-photon microscopies.

Once each fluorescent probe in a sample can be imaged individually, its positions can be determined to high precision by finding the center of the single-molecule image (Thompson et al., 2002; Yildiz et al., 2003). The uncertainty in determining the molecule's position (i.e., the localization precision) scales approximately with the inverse square root of the number of photons detected from the molecule. It can be approximated by $\bar{a} \approx \Delta/\sqrt{N}$, wherein Δ denotes the width of the diffraction-limited point spread function and N is the number of photons detected

(Thompson et al., 2002). For bright fluorescent dyes, about one million photons can be detected from a single molecule, leading to a localization precision of $\leq$ 1 nm (Pertsinidis et al., 2010; Yildiz et al., 2003). The relative position of multiple fluorophores can also be determined by taking advantage of different emission colors (Churchman et al., 2005; Lacoste et al., 2000; van Oijen et al., 1998), the sequential photobleaching of individual fluorophores (Gordon et al., 2004; Qu et al., 2004), or the stochastic blinking of quantum dots (Lagerholm et al., 2006; Lidke et al., 2005).

In the literature, the localization precision is often reported as the standard deviation of multiple localization measurements of a single object, whereas both standard deviation and full width at half maximum (=2.35 × standard deviation for a Gaussian distribution) have been used as measures of the resolution. In this Primer, we use full width at half maximum to describe resolution because it illustrates better the closest resolvable separation between objects.

Stochastic Switching Enables Super-Resolution Imaging
Being able to localize a single molecule does not directly translate into super-resolution imaging of a fluorescently labeled biological sample, which can contain thousands of fluorophores inside of the diffraction-limited region. The fluorescence emission from these molecules will overlap severely enough that the overall image appears as a completely featureless blur. At first sight, it might seem impossible to distinguish these molecules individually. However, if the fluorescence emission from these molecules is controlled such that only one molecule is emitting at a time, individual molecules can then be imaged and localized. This is the idea behind a recently developed super-resolution imaging method called STORM (Rust et al., 2006), PALM (Betzig et al., 2006), or FPALM (Hess et al., 2006).

In this method, photoswitchable (or photoactivatable) fluorophores are used to achieve temporal control of the emission. These fluorophores can be converted between a fluorescent (or "on") state and a dark (or "off") state or states that fluoresce at different wavelengths. Therefore, when activation light of a sufficiently low intensity is applied to the sample, only a random, sparse subset of fluorophores is activated to the on state at any time, allowing these molecules to be imaged individually, precisely localized, and then deactivated by switching to a reversible dark state or permanent bleaching. Iterating this process—activation, imaging, and deactivation—then allows the locations of many fluorophores to be mapped and a super-resolution image constructed from these localizations (Figure 3A), either with synchronized activation (Betzig et al., 2006; Hess et al., 2006; Rust et al., 2006) or with asynchronous activation (Egner et al., 2007). The image resolution is then no longer limited by diffraction but instead by how precisely each fluorophore is localized. Using this approach, a lateral image resolution as high as $\sim$20 nm has been achieved (Rust et al., 2006).

Although photoswitching offers the most versatile strategy for achieving the temporal control needed for super-resolution imaging, other strategies can also achieve similar control in certain biological samples, such as through the binding and dissociation of fluorescent molecules (Sharonov and Hochstrasser, 2006). It is possible to obtain subdiffraction limit image resolution even when the single-molecule imaging condition is not rigorously
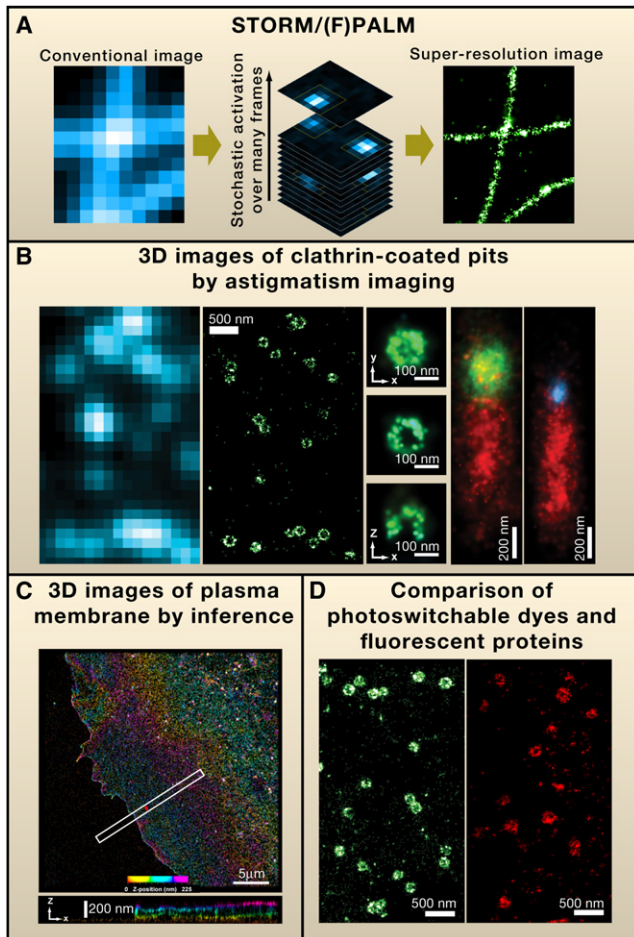
Figure 3. Super-Resolution Fluorescence Microscopy by Single-Molecule Switching

(A) This super-resolution approach takes advantage of photoswitching of fluorophores to temporally separate images of single molecules that overlap spatially. At any time during image acquisition, only a sparse subset of fluorophores is activated to the fluorescence state, allowing these molecules to be imaged individually and thus localized. After multiple iterations of the activation and imaging processes, a super-resolution image is constructed from the localizations of many fluorophores.

(B) 3D super-resolution images taken using an astigmatism approach with cylindrical lens. (Two far-left columns) Conventional image of clathrin-coated pits in a mammalian cell immunostained against clathrin, in comparison with the corresponding 3D super-resolution image showing an xy cross section near the plasma membrane. (Middle) Magnified super-resolution images of a single clathrin-coated pit in a cell-free reconstitution system with an xy projection (top), an xy cross-section at the lower portion of the pit (middle), and an xz cross section cutting through the middle of the pit (bottom). (Two far-right columns) Composite 3D image of clathrin (green), dynamin (cyan), and an F-BAR domain protein FBP17 (red) in the cell-free system. Shown here is the super-position of 59 images of clathrin and FBP17 aligned to the center of the clathrin-coated regions (left) and the super-position of 96 dynamin-FBP17 images aligned to the center of dynamin spot (right). Clathrin is directly labeled, whereas dynamin and FBP17 are immunolabeled. From Huang et al., 2008 and Wu et al., 2010. Reprinted with the permission from AAAS.

(C) 3D super-resolution images taken using an interferometry approach with apposing objectives. (Top) xy projection of the plasma membrane of a cell expressing membrane-targeting photoactivatable Eos-fluorescent protein. The color of the localization points encodes their z coordinates. (Bottom) xz cross-section of the boxed region in the top panel. Images adapted from Shtengel et al., 2009.

(D) Comparison of STORM/(F)PALM images of clathrin-coated pits immunostained with the photoswitchable Alexa647 dye (green) or tagged with the mEos2 fluorescent protein (red).

satisfied. When the density of fluorophores is not too high, such that temporal fluctuations of neighboring pixels are distinct, higher-order correlation analysis of the temporal fluctuations of individual pixels can be used to substantially improve the image resolution (Dertinger et al., 2009).

Fluorescent Probes

The requirements of STORM/(F)PALM put several constraints on the fluorescent probes. First, the probes should have a fluorescent state that emits light at a certain range of wavelengths and a "dark" state that does not emit light in this wavelength range. Second, to achieve high precision of localization, the probes should emit a large number of photons before going dark. Third, because only one fluorophore is activated within a diffraction-limited area at any time and the vast majority of fluorophores remain in the dark state, dark state emission should be minimal to ensure high-precision localization of the activated molecule. Finally, because all switchable fluorophores can be spontaneously activated by thermal energy or by the imaging laser (as opposed to the activation laser), this spontaneous activation could cause more than one fluorophore in the diffraction limited area to be turned on even without activation light, preventing single-molecule detection. Therefore, a low spontaneous activation rate is also desired.

Despite these requirements, a large number of switchable fluorophores have been used for STORM/(F)PALM imaging (Huang et al., 2009; Patterson et al., 2010). These probes range from organic dyes to fluorescent proteins (Table S1 available online), allowing the labeling of biological samples with a variety of methods and in multiple colors. To provide readers with general guidelines for choosing the appropriate fluorophore, we describe the advantages and disadvantages of several switchable fluorophores in the Supplemental Information.

For specific experiments, the decision of whether to use dyes or fluorescent proteins depends on a variety of factors, which are commonly applicable to all fluorescence imaging methods. In terms of labeling, fluorescent proteins are genetically encodable, allowing proteins in living cells to be readily labeled with fluorescent proteins. However, dyes are more versatile for labeling different molecular species, including proteins, nucleic acids, oligosaccharides, and even small molecules. Tagging cellular proteins with dyes is typically achieved using immunofluorescence, which permits endogenously expressed proteins to be labeled but prohibits most live-cell imaging applications. In terms of the optical properties, dyes generally have a significantly higher photon output, allowing higher image resolution than fluorescent proteins (Figure 3D). However, at extremely high image resolution, the bulky size of the antibody (10–15 nm) could limit image resolution when immunofluorescence labeling is used. Therefore, the recently developed hybrid fusion systems provide a promising solution that combines the merits of both genetic encoding and the superior fluorescence properties of organic dyes (Fernández-Suárez and Ting, 2008). In these approaches, the protein of interest is fused to a marker protein or peptide, which in turn exhibits a specific reactivity or affinity to fluorescent dyes with certain reactive groups.

3D Imaging

By determining the position of individual molecules in all three dimensions, super-resolution microscopy based on

single-molecule switching can be extended to 3D. The first implementation of this approach uses a simple optical design that takes advantage of astigmatism in which light propagating in perpendicular planes has different focal points. Specifically, a cylindrical lens is inserted in the imaging path, such that the shape of a single-molecule image becomes elliptical. This makes it possible to determine the axial position of the molecule from the ellipticity and the lateral position from the center position of the image (Huang et al., 2008).Figure 3B shows 3D images of clathrin-coated pits taken with this approach, resolving the nanomorphology of these structures (Huang et al., 2008). Other implementations have utilized a variety of 3D localization methods, such as capturing defocused images at two different focal planes (Juette et al., 2008), engineering a PSF with a double-helical shape (Pavani et al., 2009), and using a mirror to project the axial view to the lateral direction (Tang et al., 2010). Axial resolutions of 40–70 nm have been reported using these methods.

The highest axial resolution in 3D STORM/(F)PALM is achieved by interferometry using two opposing objectives in a similar fashion to 4Pi microscopy and I^5M (Shtengel et al., 2009). Figure 2C shows the clear separation of the ventral and dorsal plasma membrane in a thin protrusion of the cell using this method, demonstrating a z resolution of 10 nm (Shtengel et al., 2009). The imaging depth of this approach is relatively small compared to the PSF-fitting approaches described in the previous paragraph, but sample scanning can increase the imaging depths of all of these approaches. In practice, the imaging depth is limited by spherical aberrations due to refractive index mismatch, scattering by turbid samples, and high-fluorescence background arising from thick samples. The combination of single-molecule-based super-resolution imaging with two-photon excitation/activation provides a promising solution to the latter two problems (Fölling et al., 2008; Vaziri et al., 2008).

Live-Cell Imaging

As with STED and SIM, there is also a trade-off between spatial and temporal resolution with STORM/(F)PALM imaging. In this case, the image is reconstructed from single-molecule localizations. When specifying the spatial resolution, a Nyquist resolution (defined as twice the average distance between neighboring localizations) should be considered in addition to the localization precision (Shroff et al., 2008). This consideration effectively limits the temporal resolution to the time required to collect enough localizations to give the desired Nyquist resolution.

A time resolution of 25–60 s per frame was obtained when imaging focal adhesion complexes labeled with Eos fluorescent protein (EosFP) at a Nyquist resolution of 60–70 nm (Shroff et al., 2008). Similar spatial and temporal resolutions have been achieved when studying the cytoskeleton structure in bacteria using enhanced yellow fluorescent protein (EYFP) (Biteen et al., 2008). This relatively slow imaging speed is due, in part, to the slow switching of fluorescent proteins to the dark states but also due to the decreasing photon output at high-excitation intensities. The use of brighter and faster-switching organic dyes could potentially increase the imaging speed. Various dyes have been combined with the hybrid fusion systems for live-cell super-resolution imaging (Lee et al., 2010; Testa et al., 2010;

Wombacher et al., 2010). The spatiotemporal resolution that can be reached with photoswitchable dyes has yet to be characterized with the Nyquist criteria.

Photoactivation has also been combined elegantly with single-particle tracking to visualize dynamic events of living cells (Hess et al., 2007; Manley et al., 2008). Unlike conventional single-molecule tracking experiments, which require low density of target molecules, the use of photoswitchable probes allows a high density of target molecules to be labeled and tracked. Although it may still take a substantial amount of time to accumulate the large number of localizations required to define a structure with high resolution, the motion and dynamics of the molecules inside of the structures can be obtained with millisecond temporal resolution from these single-molecule traces. This imaging mode greatly extends the power of dynamic single-molecule imaging.

Applications of Super-Resolution Fluorescence Microscopy

Despite its relatively short history, super-resolution fluorescence microscopy has already been applied to many areas of biology, and it is beginning to have an impact on numerous fields. It is not possible to describe all of these applications in this Primer article. Instead, we discuss some representative examples in the areas of cell biology, microbiology, and neurobiology.

In Cell Biology

During the development of super-resolution microscopy techniques, a number of subcellular structures with well-characterized morphological features were frequently chosen as proof-of-principle model systems, including microtubules, actin, clathrin-coated pits, mitochondria, endoplasmic reticulum, and focal adhesion complexes. These studies have not only illustrated the resolving power of the new super-resolution techniques, but they also demonstrated these methods' potential for visualizing molecular structures and interactions in cells.

One particularly promising area of applying super-resolution microscopy techniques is the investigation of plasma membrane proteins and membrane microdomains. These domains are generally too small to be resolved by conventional light microscopy. Indeed, many of the controversies in this field, such as the size and the life time of lipid rafts, are due to the lack of direct observations of these microdomains. Super-resolution microscopy thus offers a powerful tool to resolve these debates.

For example, STED microscopy has resolved individual syntaxin 1 clusters in cells, allowing the quantification of the number of syntaxin molecules per cluster (~90) and cluster size (50–60 nm) (Sieber et al., 2007). In conjunction with diffusion measurements by fluorescence recovery after photobleaching (FRAP) and computer modeling, STED demonstrates that syntaxin self-association and steric repulsion fully explain the size and dynamics of syntaxin clusters. In contrast, the clustering of nicotinic acetylcholine receptors is possibly affected by additional mechanisms, including cholesterol-mediated protein-protein interactions and cytoskeleton membrane-protein interactions. These results provide an explanation for the observation that the depletion of cholesterol influences both short range (~50 nm) and long range (0.5–3.5 μm) organizations of nicotinic acetylcholine receptors (Kellner et al., 2007).

The dynamic nature of membrane components requires live-cell imaging with high time resolution. Photoactivation-facilitated high-density single-particle tracking provides a powerful approach to study these dynamics on millisecond to second time scales. Studies of influenza hemagglutinin (Hess et al., 2007), HIV Gag protein, vesicular stomatitis virus G protein (VSVG) (Manley et al., 2008), and epidermal growth factor receptor (Subach et al., 2009, 2010) have uncovered heterogeneous clustering and diffusion behaviors of these membrane proteins. Complementary to this single-particle tracking approach, STED-FCS probes the diffusion behavior of molecules within a subdiffraction focal spot with microsecond time resolution. Studies with STED-FCS discovered that sphingolipids and GPI-anchored proteins can be briefly (10–20 ms) trapped in cholesterol-associated membrane domains of < 20 nm in size, whereas phosphoglycerolipids exhibit free diffusion (Eggeling et al., 2009).

Super-resolution imaging also allows the visualization of fine structures within membrane organelles. For example, biochemical measurements found that human voltage-dependent anion channels (hVDAC) in mitochondria membranes associate with the cytosolic hexokinase-1. In contrast, two-color STED images of mitochondria revealed that a substantial fraction of hVDAC does not colocalize with the pool of hexokinase-I bound to mitochondria. The STED images also reveal that the three hVDAC subtypes exists in distinct domains on the mitochondria outer membrane (Neumann et al., 2010). IsoSTED has resolved the cristae in the mitochondria inner membrane (Schmidt et al., 2009), suggesting the potential to study protein interactions in the interior of mitochondria.

STORM/(F)PALM has also provided new insights into the organizations of proteins associated with plasma membranes and intracellular membrane organelles. Super-resolution images taken with this approach resolved the hemispherical shape of the clathrin coat on nascent endocytic vesicles (Figure 3B) (Bates et al., 2007; Huang et al., 2008). In an in vitro endocytosis model system, two-color 3D imaging revealed that the two tubule-forming proteins, dynamin and the F-BAR domain protein FBP17, have distinct distributions along the membrane tubules connecting clathrin-coated pits and the basal plasma membrane (Figure 3B) . In addition, super-resolution imaging, combined with electron microscopy and time-lapse conventional fluorescence imaging, uncovered an unexpected role of FBP17 in creating endocytic vesicles (Wu et al., 2010). Live-cell super-resolution imaging has also revealed interesting dynamics of adhesion complexes during their initiation, maturation, and dissolution (Shroff et al., 2008). A recent 3D super-resolution study revealed a multilaminar molecular architecture of the focal adhesion core region that connects integrin and actin (Kanchanawong et al., 2010). This core region is comprised of an integrin-signaling layer, a force transduction layer, and an actin regulatory layer (Kanchanawong et al., 2010).

Super-resolution fluorescence microscopy is also expected to expand our understanding of the structures inside of the nucleus. The highly condensed DNA packaging inside of the nucleus calls for super-resolution imaging with protein and nucleic acid sequence specificity, which is difficult to achieve by any other means. Super-resolution fluorescence microscopy provides the opportunity to resolve the interactions between nucleic acids and proteins inside of the nucleus. For example, studies with 3D SIM revealed morphological changes of the chromosomes and the nuclear lamin during early mitosis (Schermelleh et al., 2008). In addition, STORM/(F)PALM has shown promise in resolving chromatin fibers (Matsuda et al., 2010). We anticipate that, with further improved image resolution and sequence-specific nucleic acid labeling by FISH, DNA/RNA-binding proteins, or aptamers, the regulation of gene expression may be directly visualized inside of the nucleus using super-resolution imaging.

These are only a few examples that illustrate the impact that super-resolution fluorescence microscopy is having on cell biology. We look forward to seeing more questions answered by the rapid adoption of super-resolution microscopy tools, especially given this technique's ability to resolve subcellular structures beyond the organelle level.

In Microbiology

Super-resolution fluorescence microscopy may be the imaging tool for which microbiologists have long been waiting. In bacteria, life processes occur in a small, crowded volume of $\sim$1 um^3, in which thousands of different protein and RNA species reside. Our view of bacterial structure has undergone a major transformation in recent years. Instead of being viewed simply as a bag of randomly distributed molecules colliding with each other, we now realize that bacteria contain highly organized chromosomes, dynamic cytoskeletal structures, and specific subcellular regions involved in signaling and biosynthetic processes. However, our understanding of the molecular organization in bacterial cells is still primitive.

This gap in our knowledge stems primarily from the difficulty in imaging such a small cell, with a size not much larger than the diffraction limit of optical resolution. Indeed, under the light microscope, most structures inside of a bacterial cell look like a blur. Though electron microscopy (EM) often comes to the rescue when high image resolution is required, its application to bacterial imaging is rather limited. To obtain molecular-specific contrast with EM, immunogold labeling is typically used, and this labeling approach requires cell fixation and permeabilization. Unfortunately, this fixation and permeabilization process perturbs structures inside of bacteria substantially more than inside of eukaryotic cells. Furthermore, live imaging is so far impossible with EM.

The high molecular specificity offered by various fluorescent labeling approaches and the live-cell compatibility of super-resolution fluorescence microscopy offer an ideal solution to the bacterial imaging problem. Indeed, this approach has been used to study several different protein organizations in bacterial cells. For example, STORM/(F)PALM was used to determined the distributions of the chemotaxis proteins Tar receptor, CheY, and CheW in fixed *Escherichia coli* cells (Greenfield et al., 2009). These proteins were found to form clusters with exponentially distributed sizes. The cluster locations were consistent with a stochastic self-assembly model that does not require active transport. In *Calobactur crescentus*, live-cell STORM/(F)PALM imaging of MreB, an actin analog, revealed a helical organization of the protein (Biteen et al., 2008). A similar approach was also used to study the partitioning (Par) apparatus

in *C. crescentus.* These studies found that the ATPase ParA forms a narrow, linear polymer structure that runs through the center of the cell body, functioning in a way that is similar to the mitotic spindles observed in eukaryotic cells (Ptacin et al., 2010).

These early applications of super-resolution imaging to bacterial cells have shown the great promise of the approach. Considering the primitive knowledge that we have of the organization of the chromosomes and proteins in bacteria, we expect super-resolution fluorescence microscopy to transform microbiology in the coming years.

In Neurobiology

Ever since Cajal observed Golgi-stained neurons under light microscopes more than a century ago, we have known that the brain functions by sending information from the axons to the dendrites of neurons. Therefore, a "wiring diagram" detailing how neurons are connected to each other will provide a structural foundation for understanding brain function, as well as its malfunction in some neurological disorders. However, such a wiring diagram has not been obtained yet except for *Caenorhabditis elegans* (White et al., 1986). Why not? The small diameter of neurites (as small as tens of nanometers) and their high packing density require image resolution at the nanometer scale for wire tracing. Moreover, to annotate a wiring diagram, we need to identify the neuronal connections (i.e., the synapses) and characterize their properties. These properties depend on the molecular content of the synapses and thus require imaging with molecular specificity. In fact, synaptic function is orchestrated by an elaborate protein machinery with hundreds of protein species packed together in a structure of submicron size. Understanding synaptic function and plasticity requires a detailed characterization of the organization and dynamics of these molecules at specific synaptic sites. Thus, a method to map neural circuitry needs molecule-specific contrast, nanometer-scale resolution, and, ideally, live tissue imaging capability. Super-resolution fluorescence microscopy uniquely satisfies these requirements.

Indeed, neuroscience is one of the first disciplines to which super-resolution fluorescence microscopy was applied. One productive area of application is the study of subneuronal structures, such as synapses. STED images of the active zone protein Bruchpilot at the neuromuscular junction in *Drosophila* revealed a donut-shaped distribution centered at the active zones of the synapses. Furthermore, the molecules appear to adopt a preferred orientation along the transynaptic axis (Fouquet et al., 2009; Kittel et al., 2006). Using a similar approach, AMPA receptors have been shown to have a ring-shaped distribution in the ribbon synapses of inner hair cells (Meyer et al., 2009). Studies of synaptotagmin, a component of the synaptic vesicle component, show that these proteins remain clustered after exocytosis (Willig et al., 2006).

STORM/(F)PALM has also been used to investigate the molecular architecture of synapses. A systematic study of ten pre- and postsynaptic proteins in the central synapses of mouse brain tissue revealed oriented organization of the presynaptic scaffolding proteins bassoon and piccolo; compartmental distributions of the postsynaptic proteins PSD95, shank, and Homer; and heterogeneous neurotransmitter receptor distributions,

with some synapses showing central-synaptic and others showing perisynaptic receptor distribution (Dani et al., 2010). The molecule counting capability of this approach allowed quantitative analysis of neurotransmitter receptor compositions in synapses (Dani et al., 2010). One recent study adapted photoactivation-facilitated high-density single-particle tracking to study actin dynamics at the dendritic spine and uncovered distinct loci of enhanced actin polymerization (Frost et al., 2010).

In addition to illuminating subcellular structures inside of neurons, super-resolution fluorescence microscopy has also been used to study neuronal morphology. Beautiful STED images revealed the shape and dynamics of dendritic spines in live cells (Nägerl et al., 2008). Two-photon STED allowed the visualization of spine morphology in deep tissue samples (Ding et al., 2009). The application of super-resolution imaging to map neuronal connectivity is also currently under way.

However, determining the complete neuronal wiring diagram may require even higher resolution than what is currently feasible by super-resolution microscopy. Although resolution of a few tens of nanometers is now routinely obtainable using various super-resolution fluorescence microscopy techniques, tracing thin and densely packed axons in the brain may require a resolution of a few nanometers. Studying subneuronal structures, such as synapses, could also benefit from substantially higher resolution than the current state of the art. A resolution of a few tens of nanometers allows the organization of molecular assemblies and organelles to be determined, whereas resolution at a few nanometers (i.e., a true molecular scale) would permit the direct visualization of interactions between molecules.

Concluding Remarks

Not that long ago, the diffraction limit was considered insurmountable. In recent years, the invention of various super-resolution techniques has shattered the diffraction barrier and allowed the resolution of images from light microscopy to improve by an order of magnitude over the diffraction limit. In fact, all of these super-resolution approaches have, in principle, made spatial resolution unlimited. That said, we believe that, practically, an additional order of magnitude in resolution improvement is feasible.

It is worth noting that, in addition to the intrinsic optical resolution, which often depends on the brightness and photostability of the fluorescent probes, the effective image resolution is also limited by the labeling density and the size of the fluorescent labels. Therefore, in addition to improvements in the design of microscopes, developments in fluorescent probes and labeling chemistry are also critical for further improving the resolution of light microscopy. Indeed, recent advances in super-resolution fluorescence microscopy have already inspired a large amount of research activity in these areas. We foresee that, together, these efforts will allow imaging at a truly molecular-scale resolution, thereby enabling the direct visualization of molecular interactions and biochemical events in living cells.

REFERENCES

Abbe, E. (1873). Beitrage zur Theorie des Mikroskops und der mikroskopischen Wahrnehmung. Arch. Mikroskop Anat. *9*, 413–420.

Bates, M., Huang, B., Dempsey, G.T., and Zhuang, X.W. (2007). Multicolor super-resolution imaging with photo-switchable fluorescent probes. Science *317*, 1749–1753.

Betzig, E., Lewis, A., Harootunian, A., Isaacson, M., and Kratschmer, E. (1986). Near-field scanning optical microscopy (NSOM) - Development and biophysical applications. Biophys. J. *49*, 269–279.

Betzig, E., Patterson, G.H., Sougrat, R., Lindwasser, O.W., Olenych, S., Bonifacino, J.S., Davidson, M.W., Lippincott-Schwartz, J., and Hess, H.F. (2006). Imaging intracellular fluorescent proteins at nanometer resolution. Science *313*, 1642–1645.

Biteen, J.S., Thompson, M.A., Tselentis, N.K., Bowman, G.R., Shapiro, L., and Moerner, W.E. (2008). Super-resolution imaging in live Caulobacter crescentus cells using photoswitchable EYFP. Nat. Methods *5*, 947–949.

Bretschneider, S., Eggeling, C., and Hell, S.W. (2007). Breaking the diffraction barrier in fluorescence microscopy by optical shelving. Phys. Rev. Lett. *98*, 218103.

Churchman, L.S., Okten, Z., Rock, R.S., Dawson, J.F., and Spudich, J.A. (2005). Single molecule high-resolution colocalization of Cy3 and Cy5 attached to macromolecules measures intramolecular distances through time. Proc. Natl. Acad. Sci. USA *102*, 1419–1423.

Dani, A., Huang, B., Bergan, J., Dulac, C., and Zhuang, X. (2010). Super-resolution imaging of chemical synapses in the brain. Neuron *68*, 843–856.

Dertinger, T., Colyer, R., Iyer, G., Weiss, S., and Enderlein, J. (2009). Fast, background-free, 3D super-resolution optical fluctuation imaging (SOFI). Proc. Natl. Acad. Sci. USA *106*, 22287–22292.

Ding, J.B., Takasaki, K.T., and Sabatini, B.L. (2009). Supraresolution imaging in brain slices using stimulated-emission depletion two-photon laser scanning microscopy. Neuron *63*, 429–437.

Donnert, G., Keller, J., Wurm, C.A., Rizzoli, S.O., Westphal, V., Schönle, A., Jahn, R., Jakobs, S., Eggeling, C., and Hell, S.W. (2007). Two-color far-field fluorescence nanoscopy. Biophys. J. *92*, L67–L69.

Eggeling, C., Ringemann, C., Medda, R., Schwarzmann, G., Sandhoff, K., Polyakova, S., Belov, V.N., Hein, B., von Middendorff, C., Schönle, A., and Hell, S.W. (2009). Direct observation of the nanoscale dynamics of membrane lipids in a living cell. Nature *457*, 1159–1162.

Egner, A., Geisler, C., von Middendorff, C., Bock, H., Wenzel, D., Medda, R., Andresen, M., Stiel, A.C., Jakobs, S., Eggeling, C., et al. (2007). Fluorescence nanoscopy in whole cells by asynchronous localization of photoswitching emitters. Biophys. J. *93*, 3285–3290.

Fernández-Suárez, M., and Ting, A.Y. (2008). Fluorescent probes for super-resolution imaging in living cells. Nat. Rev. Mol. Cell Biol. *9*, 929–943.

Fölling, J., Belov, V., Riedel, D., Schönle, A., Egner, A., Eggeling, C., Bossi, M., and Hell, S.W. (2008). Fluorescence nanoscopy with optical sectioning by two-photon induced molecular switching using continuous-wave lasers. ChemPhysChem *9*, 321–326.

Fouquet, W., Owald, D., Wichmann, C., Mertel, S., Depner, H., Dyba, M., Hallermann, S., Kittel, R.J., Eimer, S., and Sigrist, S.J. (2009). Maturation of active zone assembly by Drosophila Bruchpilot. J. Cell Biol. *186*, 129–145.

Frost, N.A., Shroff, H., Kong, H., Betzig, E., and Blanpied, T.A. (2010). Single-molecule discrimination of discrete perisynaptic and distributed sites of actin filament assembly within dendritic spines. Neuron *67*, 86–99.

Giepmans, B.N., Adams, S.R., Ellisman, M.H., and Tsien, R.Y. (2006). The fluorescent toolbox for assessing protein location and function. Science *312*, 217–224.

Gordon, M.P., Ha, T., and Selvin, P.R. (2004). Single-molecule high-resolution imaging with photobleaching. Proc. Natl. Acad. Sci. USA *101*, 6462–6465.

Greenfield, D., McEvoy, A.L., Shroff, H., Crooks, G.E., Wingreen, N.S., Betzig, E., and Liphardt, J. (2009). Self-organization of the Escherichia coli chemotaxis network imaged with super-resolution light microscopy. PLoS Biol. *7*, e1000137.

Gustafsson, M.G.L. (2000). Surpassing the lateral resolution limit by a factor of two using structured illumination microscopy. J. Microsc. *198*, 82–87.

Gustafsson, M.G.L. (2005). Nonlinear structured-illumination microscopy: wide-field fluorescence imaging with theoretically unlimited resolution. Proc. Natl. Acad. Sci. USA *102*, 13081–13086.

Gustafsson, M.G.L., Agard, D.A., and Sedat, J.W. (1995). Sevenfold improvement of axial resolution in 3D wide-field microscopy using two objective lenses. Proc. SPIE *2412*, 147–156.

Gustafsson, M.G.L., Shao, L., Carlton, P.M., Wang, C.J.R., Golubovskaya, I.N., Cande, W.Z., Agard, D.A., and Sedat, J.W. (2008). Three-dimensional resolution doubling in wide-field fluorescence microscopy by structured illumination. Biophys. J. *94*, 4957–4970.

Harke, B., Ullal, C.K., Keller, J., and Hell, S.W. (2008). Three-dimensional nanoscopy of colloidal crystals. Nano Lett. *8*, 1309–1313.

Heintzmann, R., and Cremer, C. (1999). Lateral modulated excitation microscopy: improvement of resolution by using a diffraction grating. Proc. SPIE *3568*, 185–196.

Heintzmann, R., and Gustafsson, M.G.L. (2009). Subdiffraction resolution in continuous samples. Nat. Photonics *3*, 362–364.

Heintzmann, R., Jovin, T.M., and Cremer, C. (2002). Saturated patterned excitation microscopy—a concept for optical resolution improvement. J. Opt. Soc. Am. A Opt. Image Sci. Vis. *19*, 1599–1609.

Hell, S.W. (2003). Toward fluorescence nanoscopy. Nat. Biotechnol. *21*, 1347–1355.

Hell, S.W. (2007). Far-field optical nanoscopy. Science *316*, 1153–1158.

Hell, S.W., and Stelzer, E.H.K. (1992). Fundamental improvement of resolution with 4Pi-confocal fluorescence microscope using 2-photon excitation. Opt. Commun. *93*, 277–282.

Hell, S.W., and Wichmann, J. (1994). Breaking the diffraction resolution limit by stimulated emission: stimulated-emission-depletion fluorescence microscopy. Opt. Lett. *19*, 780–782.

Hess, S.T., Girirajan, T.P.K., and Mason, M.D. (2006). Ultra-high resolution imaging by fluorescence photoactivation localization microscopy. Biophys. J. *91*, 4258–4272.

Hess, S.T., Gould, T.J., Gudheti, M.V., Maas, S.A., Mills, K.D., and Zimmerberg, J. (2007). Dynamic clustered distribution of hemagglutinin resolved at 40 nm in living cell membranes discriminates between raft theories. Proc. Natl. Acad. Sci. USA *104*, 17370–17375.

Hofmann, M., Eggeling, C., Jakobs, S., and Hell, S.W. (2005). Breaking the diffraction barrier in fluorescence microscopy at low light intensities by using reversibly photoswitchable proteins. Proc. Natl. Acad. Sci. USA *102*, 17565–17569.

Huang, B., Wang, W.Q., Bates, M., and Zhuang, X.W. (2008). Three-dimensional super-resolution imaging by stochastic optical reconstruction microscopy. Science *319*, 810–813.

Huang, B., Bates, M., and Zhuang, X. (2009). Super-resolution fluorescence microscopy. Annu. Rev. Biochem. *78*, 993–1016.

Juette, M.F., Gould, T.J., Lessard, M.D., Mlodzianoski, M.J., Nagpure, B.S., Bennett, B.T., Hess, S.T., and Bewersdorf, J. (2008). Three-dimensional sub-100 nm resolution fluorescence microscopy of thick samples. Nat. Methods *5*, 527–529.

Kanchanawong, P., Shtengel, G., Pasapera, A.M., Ramko, E.B., Davidson, M.W., Hess, H.F., and Waterman, C.M. (2010). Nanoscale architecture of integrin-based cell adhesions. Nature *468*, 580–584.

Kellner, R.R., Baier, C.J., Willig, K.I., Hell, S.W., and Barrantes, F.J. (2007). Nanoscale organization of nicotinic acetylcholine receptors revealed by stimulated emission depletion microscopy. Neuroscience *144*, 135–143.

Kittel, R.J., Wichmann, C., Rasse, T.M., Fouquet, W., Schmidt, M., Schmid, A., Wagh, D.A., Pawlu, C., Kellner, R.R., Willig, K.I., et al. (2006). Bruchpilot promotes active zone assembly, Ca2+ channel clustering, and vesicle release. Science *312*, 1051–1054.

Klar, T.A., and Hell, S.W. (1999). Subdiffraction resolution in far-field fluorescence microscopy. Opt. Lett. *24*, 954–956.

Kner, P., Chhun, B.B., Griffis, E.R., Winoto, L., and Gustafsson, M.G. (2009). Super-resolution video microscopy of live cells by structured illumination. Nat. Methods *6*, 339–342.

Lacoste, T.D., Michalet, X., Pinaud, F., Chemla, D.S., Alivisatos, A.P., and Weiss, S. (2000). Ultrahigh-resolution multicolor colocalization of single fluorescent probes. Proc. Natl. Acad. Sci. USA *97*, 9461–9466.

Lagerholm, B.C., Averett, L., Weinreb, G.E., Jacobson, K., and Thompson, N.L. (2006). Analysis method for measuring submicroscopic distances with blinking quantum dots. Biophys. J. *91*, 3050–3060.

Lee, H.L., Lord, S.J., Iwanaga, S., Zhan, K., Xie, H., Williams, J.C., Wang, H., Bowman, G.R., Goley, E.D., Shapiro, L., et al. (2010). Superresolution imaging of targeted proteins in fixed and living cells using photoactivatable organic fluorophores. J. Am. Chem. Soc. *132*, 15099–15101.

Lewis, A., Isaacson, M., Harootunian, A., and Muray, A. (1984). Development of a 500 Å spatial resolution light microscope. Ultramicroscopy *13*, 227–231.

Lidke, K.A., Rieger, B., Jovin, T.M., and Heintzmann, R. (2005). Superresolution by localization of quantum dots using blinking statistics. Opt. Express *13*, 7052–7062.

Lord, S.J., Lee, H.L., and Moerner, W.E. (2010). Single-molecule spectroscopy and imaging of biomolecules in living cells. Anal. Chem. *82*, 2192–2203.

Manley, S., Gillette, J.M., Patterson, G.H., Shroff, H., Hess, H.F., Betzig, E., and Lippincott-Schwartz, J. (2008). High-density mapping of single-molecule trajectories with photoactivated localization microscopy. Nat. Methods *5*, 155–157.

Matsuda, A., Shao, L., Boulanger, J., Kervrann, C., Carlton, P.M., Kner, P., Agard, D., and Sedat, J.W. (2010). Condensed mitotic chromosome structure at nanometer resolution using PALM and EGFP- histones. PLoS ONE *5*, e12768.

Meyer, A.C., Frank, T., Khimich, D., Hoch, G., Riedel, D., Chapochnikov, N.M., Yarin, Y.M., Harke, B., Hell, S.W., Egner, A., and Moser, T. (2009). Tuning of synapse number, structure and function in the cochlea. Nat. Neurosci. *12*, 444–453.

Moerner, W.E. (2007). New directions in single-molecule imaging and analysis. Proc. Natl. Acad. Sci. USA *104*, 12596–12602.

Moneron, G., and Hell, S.W. (2009). Two-photon excitation STED microscopy. Opt. Express *17*, 14567–14573.

Moneron, G., Medda, R., Hein, B., Giske, A., Westphal, V., and Hell, S.W. (2010). Fast STED microscopy with continuous wave fiber lasers. Opt. Express *18*, 1302–1309.

Nägerl, U.V., Willig, K.I., Hein, B., Hell, S.W., and Bonhoeffer, T. (2008). Live-cell imaging of dendritic spines by STED microscopy. Proc. Natl. Acad. Sci. USA *105*, 18982–18987.

Neumann, D., Bückers, J., Kastrup, L., Hell, S.W., and Jakobs, S. (2010). Two-color STED microscopy reveals different degrees of colocalization between hexokinase-I and the three human VDAC isoforms. PMC Biophys. *3*, 4.

Novotny, L., and Hecht, B. (2006). Principles of Nano-optics (Cambridge: Cambridge University Press).

Patterson, G., Davidson, M., Manley, S., and Lippincott-Schwartz, J. (2010). Superresolution imaging using single-molecule localization. Annu. Rev. Phys. Chem. *61*, 345–367.

Pavani, S.R., Thompson, M.A., Biteen, J.S., Lord, S.J., Liu, N., Twieg, R.J., Piestun, R., and Moerner, W.E. (2009). Three-dimensional, single-molecule fluorescence imaging beyond the diffraction limit by using a double-helix point spread function. Proc. Natl. Acad. Sci. USA *106*, 2995–2999.

Pertsinidis, A., Zhang, Y., and Chu, S. (2010). Subnanometre single-molecule localization, registration and distance measurements. Nature *466*, 647–651.

Pohl, D.W., Denk, W., and Lanz, M. (1984). Optical stethscopy - Image recording with resolution lembda/20. Appl. Phys. Lett. *44*, 651–653.

Ptacin, J.L., Lee, S.F., Garner, E.C., Toro, E., Eckart, M., Comolli, L.R., Moerner, W.E., and Shapiro, L. (2010). A spindle-like apparatus guides bacterial chromosome segregation. Nat. Cell Biol. *12*, 791–798.

Qu, X.H., Wu, D., Mets, L., and Scherer, N.F. (2004). Nanometer-localized multiple single-molecule fluorescence microscopy. Proc. Natl. Acad. Sci. USA *101*, 11298–11303.

Rittweger, E., Han, K.Y., Irvine, S.E., Eggeling, C., and Hell, S.W. (2009). STED microscopy reveals crystal colour centres with nanometric resolution. Nat. Photon. *3*, 144–147.

Rust, M.J., Bates, M., and Zhuang, X.W. (2006). Sub-diffraction-limit imaging by stochastic optical reconstruction microscopy (STORM). Nat. Methods *3*, 793–795.

Schermelleh, L., Carlton, P.M., Haase, S., Shao, L., Winoto, L., Kner, P., Burke, B., Cardoso, M.C., Agard, D.A., Gustafsson, M.G.L., et al. (2008). Subdiffraction multicolor imaging of the nuclear periphery with 3D structured illumination microscopy. Science *320*, 1332–1336.

Schmidt, R., Wurm, C.A., Jakobs, S., Engelhardt, J., Egner, A., and Hell, S.W. (2008). Spherical nanosized focal spot unravels the interior of cells. Nat. Methods *5*, 539–544.

Schmidt, R., Wurm, C.A., Punge, A., Egner, A., Jakobs, S., and Hell, S.W. (2009). Mitochondrial cristae revealed with focused light. Nano Lett. *9*, 2508–2510.

Sharonov, A., and Hochstrasser, R.M. (2006). Wide-field subdiffraction imaging by accumulated binding of diffusing probes. Proc. Natl. Acad. Sci. USA *103*, 18911–18916.

Shroff, H., Galbraith, C.G., Galbraith, J.A., and Betzig, E. (2008). Live-cell photoactivated localization microscopy of nanoscale adhesion dynamics. Nat. Methods *5*, 417–423.

Shtengel, G., Galbraith, J.A., Galbraith, C.G., Lippincott-Schwartz, J., Gillette, J.M., Manley, S., Sougrat, R., Waterman, C.M., Kanchanawong, P., Davidson, M.W., et al. (2009). Interferometric fluorescent super-resolution microscopy resolves 3D cellular ultrastructure. Proc. Natl. Acad. Sci. USA *106*, 3125–3130.

Sieber, J.J., Willig, K.I., Kutzner, C., Gerding-Reimers, C., Harke, B., Donnert, G., Rammner, B., Eggeling, C., Hell, S.W., Grubmüller, H., and Lang, T. (2007). Anatomy and dynamics of a supramolecular membrane protein cluster. Science *317*, 1072–1076.

Subach, F.V., Patterson, G.H., Manley, S., Gillette, J.M., Lippincott-Schwartz, J., and Verkhusha, V.V. (2009). Photoactivatable mCherry for high-resolution two-color fluorescence microscopy. Nat. Methods *6*, 153–159.

Subach, F.V., Patterson, G.H., Renz, M., Lippincott-Schwartz, J., and Verkhusha, V.V. (2010). Bright monomeric photoactivatable red fluorescent protein for two-color super-resolution sptPALM of live cells. J. Am. Chem. Soc. *132*, 6481–6491.

Synge, E.H. (1928). A suggested method for extending microscopic resolution into the ultra-microscopic region. Philos. Mag. *6*, 356–362.

Tang, J., Akerboom, J., Vaziri, A., Looger, L.L., and Shank, C.V. (2010). Near-isotropic 3D optical nanoscopy with photon-limited chromophores. Proc. Natl. Acad. Sci. USA *107*, 10068–10073.

Testa, I., Wurm, C.A., Medda, R., Rothermel, E., von Middendorf, C., Fölling, J., Jakobs, S., Schönle, A., Hell, S.W., and Eggeling, C. (2010). Multicolor fluorescence nanoscopy in fixed and living cells by exciting conventional fluorophores with a single wavelength. Biophys. J. *99*, 2686–2694.

Thompson, R.E., Larson, D.R., and Webb, W.W. (2002). Precise nanometer localization analysis for individual fluorescent probes. Biophys. J. *82*, 2775–2783.

van Oijen, A.M., Kohler, J., Schmidt, J., Muller, M., and Brakenhoff, G.J. (1998). 3-Dimensional super-resolution by spectrally selective imaging. Chem. Phys. Lett. *292*, 183–187.

Vaziri, A., Tang, J., Shroff, H., and Shank, C.V. (2008). Multilayer three-dimensional super resolution imaging of thick biological samples. Proc. Natl. Acad. Sci. USA *105*, 20221–20226.

Westphal, V., Lauterbach, M.A., Di Nicola, A., and Hell, S.W. (2007). Dynamic far-field fluorescence nanoscopy. N.J. Phys. *9*, 10.

White, J.G., Southgate, E., Thomson, J.N., and Brenner, S. (1986). The structure of the ventral nerve cord of Caenorhabditis elegans. Philos. Trans. R. Soc. Lond. B Biol. Sci. *275*, 327–348.

Willig, K.I., Rizzoli, S.O., Westphal, V., Jahn, R., and Hell, S.W. (2006). STED microscopy reveals that synaptotagmin remains clustered after synaptic vesicle exocytosis. Nature *440*, 935–939.

Willig, K.I., Harke, B., Medda, R., and Hell, S.W. (2007). STED microscopy with continuous wave beams. Nat. Methods *4*, 915–918.

Wombacher, R., Heidbreder, M., van de Linde, S., Sheetz, M.P., Heilemann, M., Cornish, V.W., and Sauer, M. (2010). Live-cell super-resolution imaging with trimethoprim conjugates. Nat. Methods *7*, 717–719.

Wu, M., Huang, B., Graham, M., Raimondi, A., Heuser, J.E., Zhuang, X., and De Camilli, P. (2010). Coupling between clathrin-dependent endocytic budding and F-BAR-dependent tubulation in a cell-free system. Nat. Cell Biol. *12*, 902–908.

Xie, X.S., Choi, P.J., Li, G.W., Lee, N.K., and Lia, G. (2008). Single-molecule approach to molecular biology in living bacterial cells. Annu. Rev. Biophys. *37*, 417–444.

Yildiz, A., Forkey, J.N., McKinney, S.A., Ha, T., Goldman, Y.E., and Selvin, P.R. (2003). Myosin V walks hand-over-hand: single fluorophore imaging with 1.5-nm localization. Science *300*, 2061–2065.

Zipfel, W.R., Williams, R.M., and Webb, W.W. (2003). Nonlinear magic: multiphoton microscopy in the biosciences. Nat. Biotechnol. *21*, 1369–1377.